Materials Today: Proceedings 42 (2021) 2789–2796

Contents lists available at ScienceDirect

Materials Today: Proceedings

journal homepage: www.elsevier.com/locate/matpr

Improvement corrosion resistance of Ni-Ti alloy by TiO_2 coating and hydroxyaptite/TiO_2 composite coating using micro arc oxidation process

Ekbal Mohammed Saeed, Nawal Mohammed Dawood, Sahar Falah Hasan

Dept. of Metallurgical Engineering, College of Materials Engineering, University of Babylon, Babylon, Iraq

ARTICLE INFO

Article history:
Available online 13 February 2021

Keywords:
Ni -Ti alloy
Nitinol
TiO_2
HA/TiO2
MAO
Corrosion resistance

ABSTRACT

Titanium oxide ceramic coatings were prepared by micro-arc oxidation (MAO) in galvanostatic regime on biomedical NiTi alloy produce via powder metallurgy, also the composite coating of HA/TiO_2 was prepared on the surface of nitinol using a one-step micro-arc oxidation (MAO), the process time for each case at 280 V was 30 min. The surface of TiO_2 coating exhibited a typical porous and rough structure. In this study, the hydroxyapatite, Ca–P precipitate it assisted to close the porous and the morphology of the surface coating showed a flower-like structure owing to the incidence of self-assembly because of the long-time of precipitate. Surface characterization of the coatings was determined utilizing SEM, XRD, and AFM. The surface morphology, topography and coating thickness were determined as well. In this study, the properties of corrosion were studied utilizing potentiostat test unit in Ringer's solution. Based on the results, the corrosion properties of NiTi alloys considerably improved due to the existence of TiO_2 and HA/TiO_2 coatings.

Selection and peer-review under responsibility of the scientific committee of the 3rd International Conference on Materials Engineering & Science.

1. Introduction

Metallic materials such as stainless steels, titanium and its alloys, cobalt alloys and nickel titanium alloy are commonly used for medical applications, because of good biocompatibility, corrosion resistance, and mechanical properties, so it has shape memory effect, super elasticity, and low density [1]. NiTi alloy is one of the most important alloys in using as a bio material due to uniqueness with properties such as, low density one and two way SMAs, superelasticity its structure and the composition is more similar for bone than other engineering materials [2]. All this and other reasons (biocompatibility) made this alloy have many uses inside the human body [3]. Generally, there are two main reasons beyond the boarder usage preventing of the NiTi alloy in the orthopedic applications as biomaterial in vascular; they are: the unexpected feature and the leaching of the nickel from the implantable devices to the tissue that surrounding it [4]. In recent years, several processes are developed for some biomaterials used for adapting the treatment of the NiTi alloy for preventing the problem of nickel releasing; however, they were not the effective solutions for that problem [5]. Some studies showed that the differences in the nickel releasing level and how that level varies with several ranges when beginning to exposure to the biological fluid until undetectable level after short time [6] and the higher concentration that last up for several months [7]. The varies in the finishing techniques are the main reason for the variations in the releasing levels of nickel. Protocols of treatments and the method of the final sterilization that used in treating processes of the NiTi alloy are considered as other reasons as well [8].

Although, metals and metal alloys that have been utilized as biomaterials behave special characteristics, modification processes of the surface were conducted to get the appropriate connection between the biomaterials and the bone tissue [9]. The modification processes of the surface were utilized for making the material's surface rougher and therefore increasing resistance against the corrosion and the biocompatibility, providing a complete integration with the bone [10], enhancing the abrasion and fatigue resistance that may arise owing to hardness increasing and creating a highly active surface from a biochemical viewpoint [11], prolonging the life and improving the material's quality [12] and decreasing the release of Ni ion from NiTi alloy biomaterials. Therefore, improving the NiTi alloy resistance against corrosion and its bioactivity by surface treatment technique is essential to make a long-lasting biomaterial [13]. A number of coating techniques have been examined for improving the properties of the surface or avoiding

E-mail addresses: mat.newal.mohammed@uobabylon.edu.iq (N.M. Dawood), Sahar.ali.math8@student.uobabylon.edu.iq (S.F. Hasan)

https://doi.org/10.1016/j.matpr.2020.12.723
2214-7853/
Selection and peer-review under responsibility of the scientific committee of the 3rd International Conference on Materials Engineering & Science.

Table 1
Specifications of Ti and Ni powders.

Material	Purity %	Average size of Particles (μm)	Source
Ti Powder	99.6	8.758	Fluke-Swiss
Ni Powder	99.7	25.835	Bucks Fluka AG Co Germany

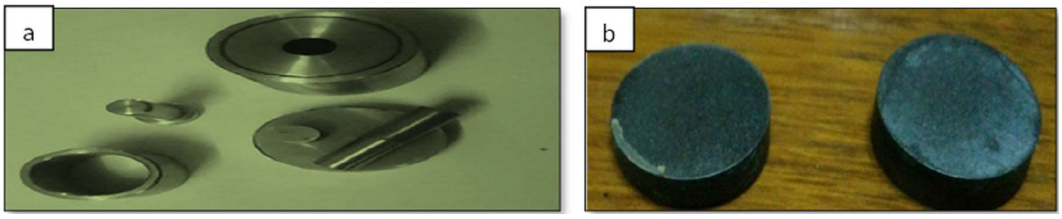

Fig. 1. a-Compaction Die, b- Samples after sintering.

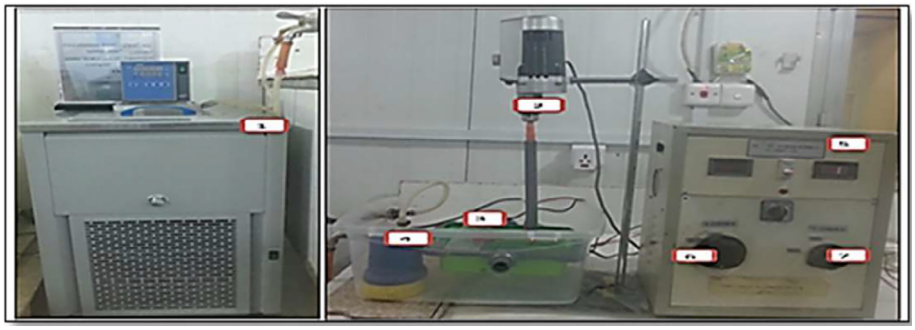

Fig. 2. Photographs of MAO coating unit.

Table 2
Prepared samples details.

Sample Code	A	B	C
Type of Coat	Uncoated	TiO_2	HA/TiO_2

Table 3
Composition of electrolytes used for MAO Process.

Sample code	B	C
Composition of electrolyte	3 g Ca, EDTA	6 g HA, 3g Ca, EDTA
Time (min)	30	30

Table 4
Chemical composition of Ringer's solution.

Substance g/l	NaCl	KCl	$CaCl_2$
Quantity	6.34	0.19	0.27

these effects like physical vapor deposition (PVD), surface oxidation, chemical vapor deposition (CVD), and ion implantation. In addition, surface properties modifying of the NiTi alloys by micro-arc oxidation (MAO) method have found increasing interest nowadays [14].

MAO method has been used widely in the recent years due to its effectiveness in preparing the oxide ceramic coatings [15]. Moreover, the NiTi alloy with Al_2O_3 coatings was prepared by MAO method that showed good resistance against corrosion and good bonding strength as well [16]. A chemical method, electrochemical deposition, or hydrothermal treating [17,18] is an inevitable consequent process required to get the HA/TiO_2 composite coating. The composite layer of HA/TiO_2 was successfully applied on the NiTi alloy utilizing a one-step MAO process [19]. There are many published studies reported that the roughness of the implant and surface area could be increased due to the presence of the composite layer, and in turn it encouraged the tissue ingrowth. Therefore, the adhesion between the implant and bone tissue was improved. Nevertheless, the composite layer formation mechanism is not clear yet. On the other hand, relatively few studies on adhesive strength between the matrix material MAO layer were conducted.

In this work, TiO_2 and HA/TiO_2 were used as coating materials on NiTi alloys using MAO method for improving the alloy's resistance against corrosion. Potentio dynamic polarization tests performed in Ringer's solution were used to determine the substrate's that coated with MAO corrosion properties. Meanwhile, SEM, XRD and AFM tests were used to determine the structural properties.

2. Materials and methods

2.1. Alloy preparation

Powder metallurgy was applied to prepare the samples from NiTi powder. The processes included mixing (Ethanol has been used as a mixing medium of wet mixing), compacting at pressure 800 MPa and sintering. Table 1 lists the purity, size of particle and origins of Ti and Ni powders utilized in this study.

For master mixture, (55 wt% Ni with 45 wt% Ti) was prepared utilizing an electric rolling mixer for 7 hr. Double action dies were used to prepare the samples with cold uniaxial pressing as shown in Fig. 1a. Electric hydraulic press with Hydraulic presser, 4387-

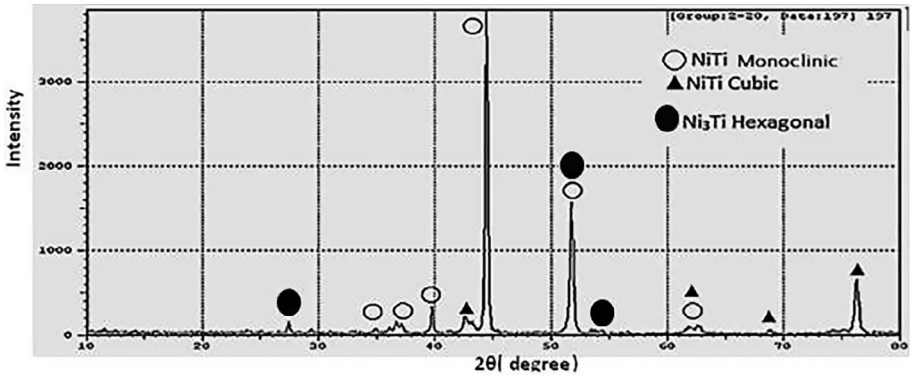

Fig. 3. XRD pattern for sample A.

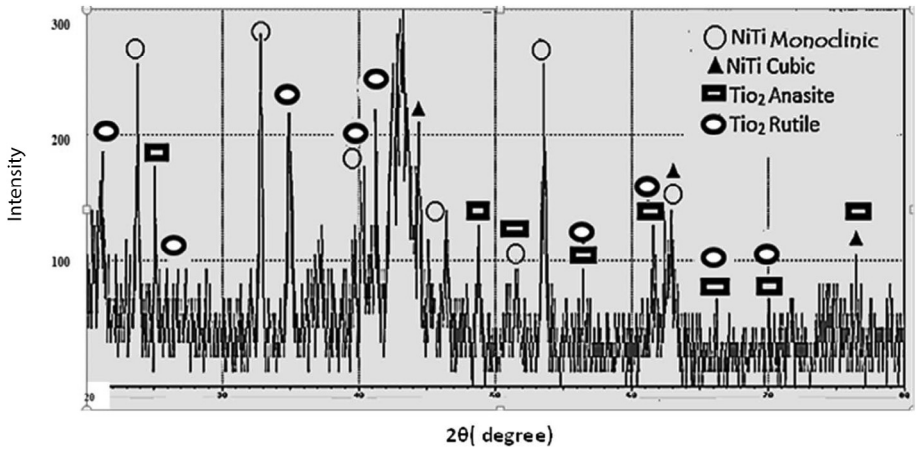

Fig. 4. XRD pattern for sample B.

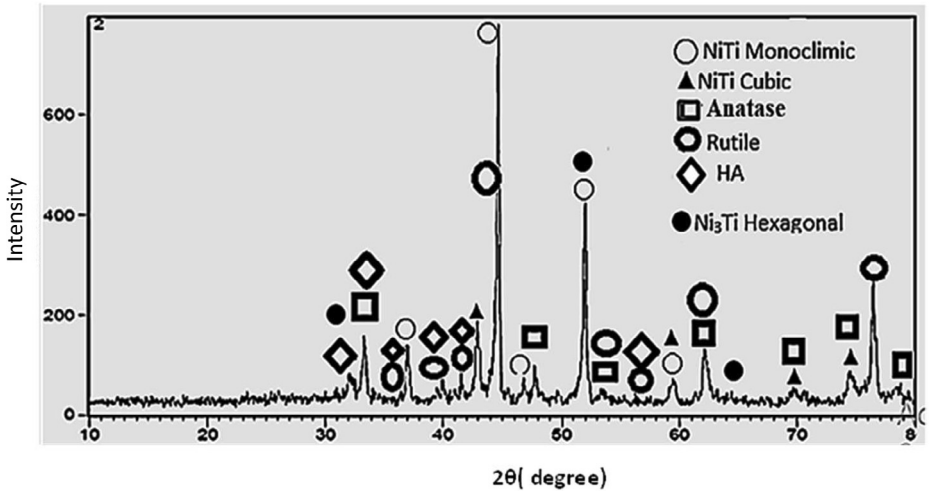

Fig. 5. XRD pattern for sample C.

4NE0000, Carver, USA was utilized to compact the green samples as disk shapes having dimensions (13.2 mm in diameter, 6.5 mm in thickness). Using 950 °C for 7 hr. and a pressure of (10^{-4} torr) with controlled argon atmosphere inside a pre-evacuated horizontal tube furnace type GSL 1600X, the samples were sintered. Fig. 1b shows the sample after sintering.

2.2. Metallographic preparation and etching

After samples sintering, wet grinded with 180, 400, 800, 1000, 1200 and 2000 grit SiC sandpapers was employed. They were polished using fine alumina (0.03 μm). Etching was made at room temperature; etching solution (10 ml of hydrofluoric acid (HF),

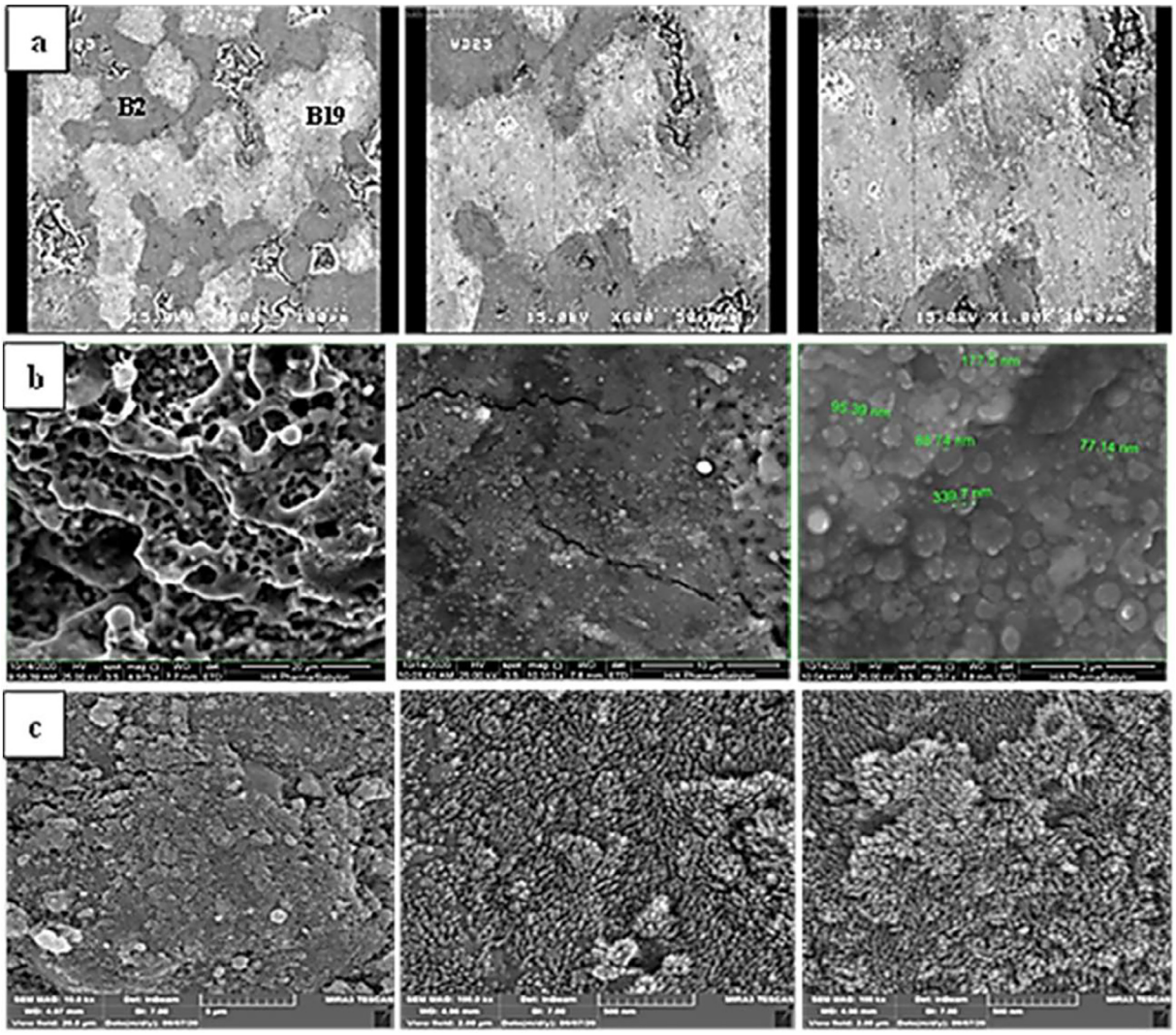

Fig. 6. SEM Micrographs of samples (a) sample A, (b) sample B, (c) and sample C.

20 ml of nitric acid (HNO_3) and 70 ml of water (H_2O)) were used [20]. Subsequently, the samples were washed using distilled water and then dried well. Using a desiccator to store the samples for the next step which is the microstructure observation.

2.3. Coating method

2.3.1. Micro arc oxidation (MAO)

After finishing the polishing process, samples were cleaned using acetone for 10 min with ultrasonic waves and then distilled water for 10 min. To form the MAO coating on the NiTi alloy, an AC-Dc power supply was utilized as shown in Fig. 2. The NiTi alloy samples were utilized as anode; however, stainless steel as a cathode. The MAO process was operated in 6 g Hydroxyapatite $Ca_{10}(PO_4)_6(OH)_2$ powder (>Ø80μm) (purity 99%) and 3 g Ca, EDTA were used in the electrolyte [21]. The PH of electrolyte solution is (8–11) [22]. The electrolyte solution was stirred and then cooled lower than 30 °C throughout the experimentation [21]. MAO was performed out at an applied voltage 280 V for a half hour because with this voltage we got a phase of $Ca_{10}(PO_4)_6(OH)_2$ and also this coating method (MAO) uses high voltages. Another sample coating at the same condition but without HA [23]. Detail description of prepared samples was shown in Table 2. After the coating, all samples were rinsed using distilled water and then dried well. Table 3 observed the composition of electrolytes used for MAO Process.

2.4. Characterization

2.4.1. XRD test

The XRD test of the NiTi alloy and the samples of coatings were tested using the system defined by (DX- 2700, XRD, using Cu Kα radiation where the value (λ = 1.5405 Å), the speed of the scanning was 5θ/min within the range of (10° to 80°) of 2θ.

2.4.2. SEM analysis

The microstructure and topography of blank and the films were examined using Scanning electron microscopy (SEM) type (FEI, Quanta 450, Czech) and combination with EDS analysis.

2.4.3. AFM analysis

The depth morphology, roughness of surface thin film was investigated with a type AA3000 Angstrom advanced Inc atomic force microscope (AFM).

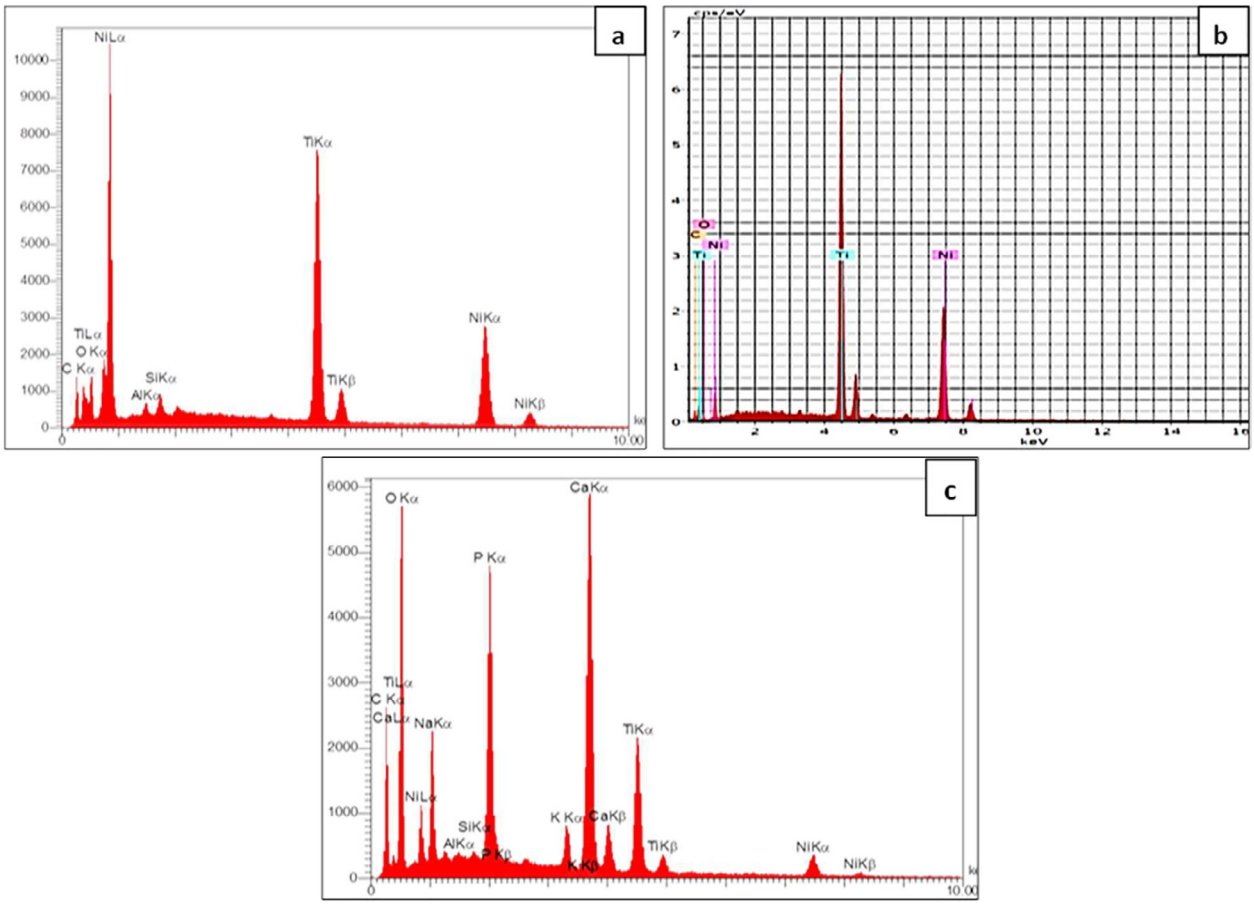

Fig. 7. EDS for (a) sample A (b) sample B and (c) sample C.

2.4.4. Thickness analysis

The film thickness measured by Microprocessor CM- 8822, coating thickness meter.

2.4.5. Hardness analysis

The test was conducted at micros Vickers hardness devices types (Digitals Micro Vickers Hardness Tester TH 717) using a load of 9.8 N for 15 sec with a squares base diamonds pyramid. The hardness was recorded as an average of five readings for each specimen.

2.5. Electrochemical test

2.5.1. Solutions

Solution used in this work Ringer's solution (Chemical Composition is shown in Table 4 with pH at 37°C was 7.4.

2.5.2. Potentiostatic polarization

The electrochemical experimental work was accomplished in a cell of three electrode that involving Ringer's solution as an electrolyte. The counter electrode was Pt electrode, and the reference electrode was SCE and working electrode (specimen) as per ASTM. The curves of the potentiodynamic polarization were presented and both corrosion current density (Icorr) and corrosion potential were found by using the Tafel plots using cathodic and anodic branches. The measurement of rate of corrosion is obtained by using Eq. (1) [24].

$$\mathbf{Corrosionrate(mpy)} = \mathbf{0.13icorr(E.W.)/A.}\rho \quad (1)$$

Where: E. W. = equivalent weight (g/ eq)

A = area measured in (cm^2)

Density measured by (g/cm^3) = ρ (after sintering)

0.13 = metric and time conversion factor

icorr. = current density ($\mu A/cm^2$).

The percentage of the improvement for the coated samples is calculated by using Eq.2 [25]:

$$\text{Improvement percentage} = (CR0\_CR/CR0)^{\times}100 \quad (2)$$

CR° and CR are the rates of corrosion of the master sample and coated samples, respectively.

3. Results and discussion

3.1. XRD results

Fig. 3 shows the pattern of the XRD for the sample A, it is observed that all Ti and Ni were transformed to the monoclinic phase of the NiTi cubic phase of the NiTi, and Ni_3Ti hexagonal phase. The slow cooling in the furnace of the samples might be considered as the main reason of the Ni_3Ti formation.

Fig. 4 shows XRD pattern after MAO of NiTi alloy. It is clear the formation of TiO_2 layer on the surface of samples in both of anatase and routile and also NiTi monoclinic, NiTi austnite and Ni_3Ti phase returne to the nitinol alloy.

Fig. 5 shows pattern of the XRD of NiTi alloy after composite coating. A composite layer HA/TiO_2 is deposited on the surface of the nitinol. The aptite layer formation is enhanced by ti-o functional group which it is produced after MAO for surface of nitinol [26].

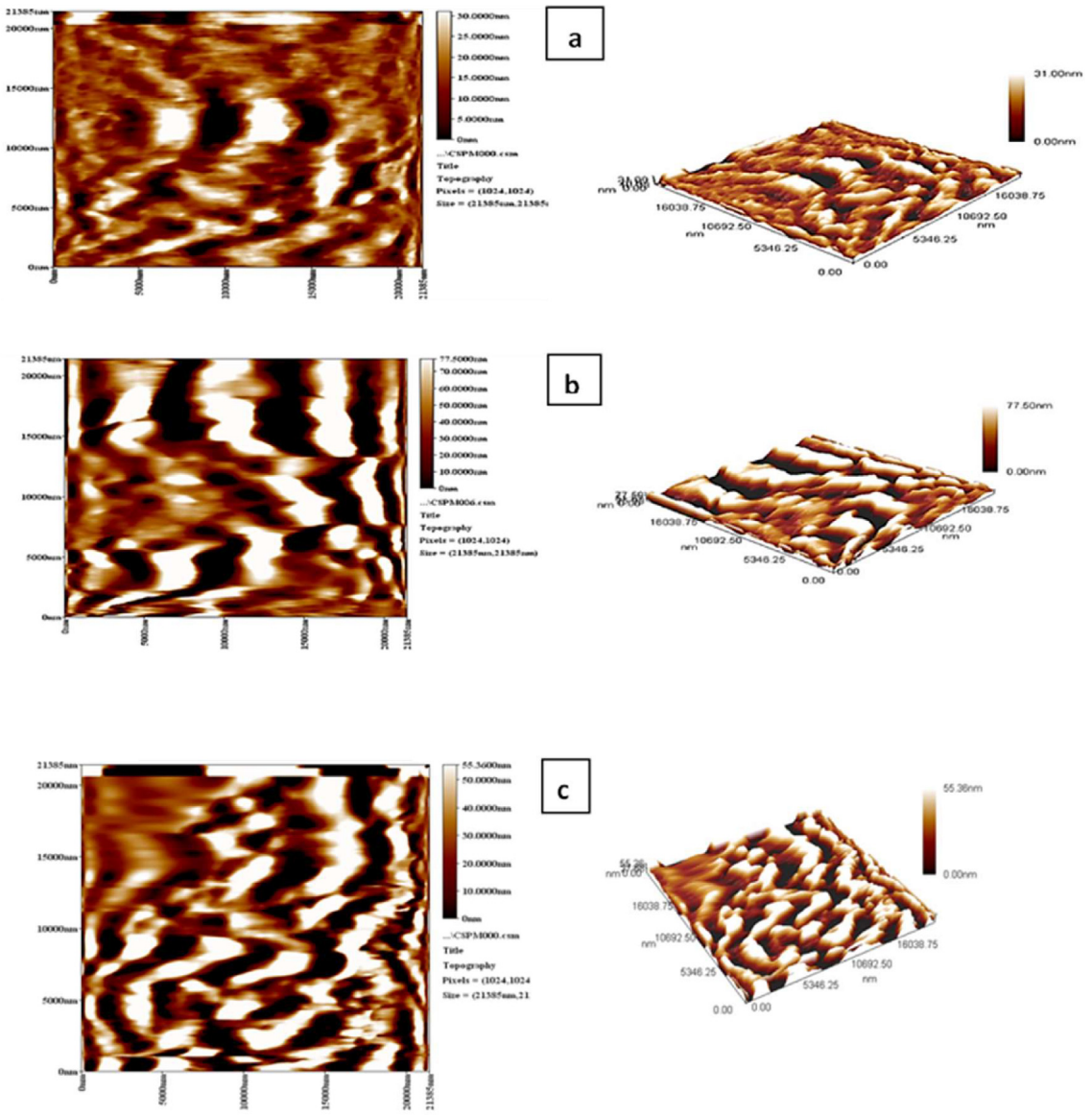

Fig. 8. AFM pattern for (a) A sample, (b) B sample and (c) C sample.

3.2. SEM and EDS results

The micrographs gained from SEM for all treated and untreated sample with MAO process are shown in Fig. 6.

Scanning electron microscope of untreated etched sample is shown in Fig. 6a. SEM images are very sensitive to chemical composition [27]. As a result, the microstructure of sintered samples showed a multi-phase structure in which the two phases (B9-NiTi and Ni3Ti) are embedded in uniformly gray matrix (NiTi-monoclinic phase B19), thus confirming XRD results.

In Fig. 6b presents the morphologies of the surface of the coating of MAO on the alloy NiTi that treated after the spark has discharged. It is noted that the resulted surface shows an outstanding MAO roughness and a structure with multiparous [23]. In addition, the melting results, plenty of circular microspores at the end interval of the formations, and plenty of micro volcano–like formations were presented in the different sizes. The pores formed in the pattern of the circle was created due to the local melting process the happen during the process of coating followed by the process of the solidification [28]. As depicted from Fig. 6b that the distributions of the uniform/non-uniform pore were observed in the nano and micro-sizes. The distribution behavior weather non-uniform or uniform was presented by the distribution of the molten material and local melting in the arc channel. The non-uniform and uniform porous structures exhibit an easier confinement and good connection with bone for the biomedical applications [29]. In Fig. 6c, the MAO coatings surface morphologies on NiTi alloy treated by hydroxyapatite was shown, Ca–P precipitate it assisted to closed the porous compared with Fig. 5b. And the morphology of the surface coating shows a structural configuration like a flower structure because of the self-assembly occurrence due to the precipitation long time of [26]. Also the homogenous precipitate led to decrease pore ratio significantly.

Fig. 7a,b and c shows the EDS spectrum of samples A, B and C respectively. As can be noticed, the EDS analysis results were comparatively closer to the addition percentage, because of that the values that gained from EDS do not consider the total area. It considers the spot where the electron stroke [27].

3.3. AFM results

Fig. 8a, b and c show results from AFM of the blank, TiO_2 and HA/TiO_2 composite coating, we observe the difference in surface topography between the samples by 3D picture to the surface.

Table 5
Sample code with surface roughness.

Sample code	A	B	C
Surface roughness (nm)	6.34	0.19	0.27

Table 6
Thickness results.

Sample code	A	B	C
Coating thickness (μm)	/	82.5	3.93

Table 7
Hardness result before and after coating.

Sample code	A	B	C
Hardness (HV)	83.25	213	187.4

Also, can be noticed from Table 5 increase of surface roughness as shown in sample (C) because of presence Ca-P precipitates closed the porous and do not allow ions pass through it [23].

3.4. Thickness test

Table 6 shows the values of layer thickness for samples B and C respectively. It is clear that sample B is much thicker than C. The formed layer of TiO_2 on the surface of nitinol is porous and growing to form multiaple layers, which explains these increasement in thickness. While HA-TiO_2 layer is homogeneous and clearly adheres to the surface.

3.5. Hardness results

Table 7 show Hardness result of the blank, TiO_2 and HA/TiO_2 composite coating, we observed that the hardness increased after MAO treatment (TiO_2 and HA/TiO_2 composite coating), these results agreement with H.R. Wanga et al. [23].

3.6. Potentiostatic - polarization test

This test was accomplished by using the Potentiostatic polarization test in the presence of Ringer's solution for uncoated, TiO_2 and HA/TiO_2 composite coated samples maintained at 37 °C as shown in Fig. 9.

Corrosion parameters (corrosion potential, corrosion current, and corrosion rate), extracted from these curves, are shown in Table 8. Fig. 9b shows the potentiodynamic polarization curves of NiTi alloy treated by MAO for 60 min in Ringer's solution. The resistance of the corrosion of the NiTi alloy is considerably increased because of the MAO treatment. This result can be confirmed by shifting of the polarization curves to the location at which the corrosion potential and corrosion current are high and low, respectively. The corrosion potential values are – 210.1 mV and – 136.3 mV for the sample A and MAO sample B, respectively. This is another indication of the increasing and improvement in the NiTi alloy when coated by oxide of the titanium formed on its surface as a result of the MAO [30]. In Fig. 9c, it could be observed that there is a significant shift toward lower current densities of the polarization curves for samples with HA/ TiO2 coating, Icorr. for sample (B) is around 0.277 μA/cm2 but at sample (C) which are much lower than Icorr around.0.01818 $\mu A/cm^2$. for (A) sample Icorr which are around 1.37μA/ cm^2. These results present the behavior of the stability of HA/TiO_2 composite coating layer. Beside the enhancement in the resistance off corrosion, this HA/TiO_2 coating is able to change the surface properties on the materials without affecting the properties of the bulk [24,31]. The corrosion current and calculated corrosion rate are relatively measure of corrosion and illustrate how much material is lost during the corrosion process. HA/TiO_2 composite coating can reduce corrosion rate of the implant of coating in human body, hence decrease release the metallic ions. The HA properties gave an advantageous application in coating of porous implants. After prostheses implantation, a contact surface between the prosthesis (metallic) and the tissue of the surrounding bone is required for sequential ingrowths of the bone. The presence of HA in the coating of the metallic implant led to a quick bonding between HA and surrounding tissue of the bone. Its application in coating implants combines the toughness and

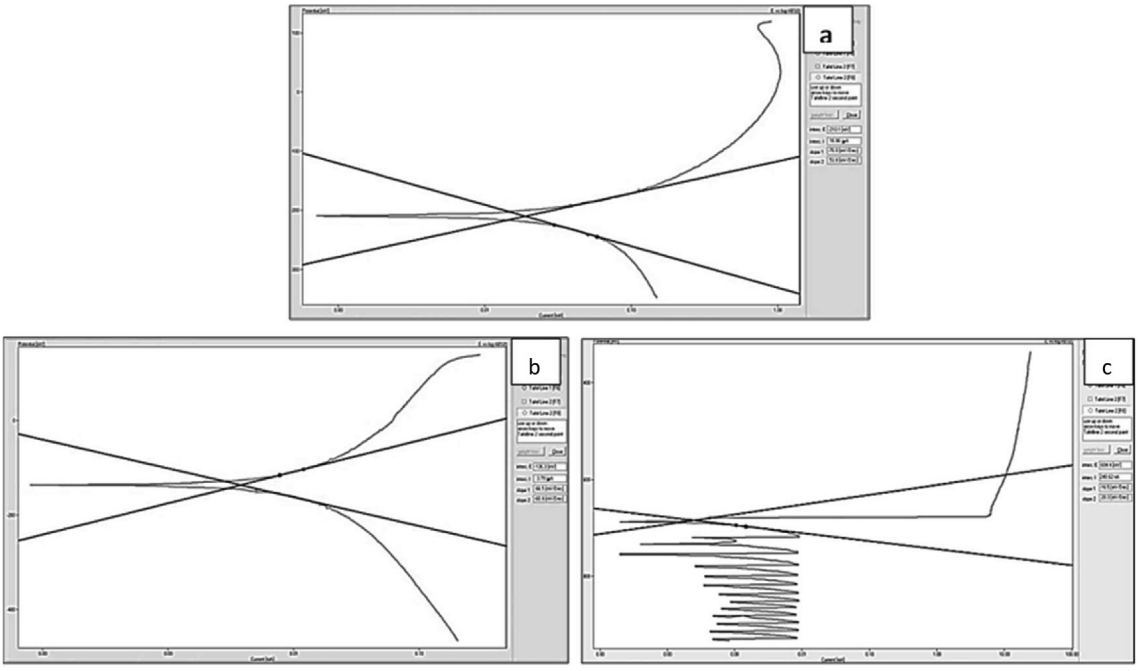

Fig. 9. Potentiostatic polarization curves for (a) A sample, (b) B sample and (c) C sample in Ringer's solution.

Table 8
Illustrate the Corrosion Potential (Ecorr.), Corrosion density (Icorr.), Corrosion Rate (CR) and Improvement Percentage of coated Samples in Ringer's solution at 37 °C.

Improvement percentage%	Corrosion rate × 10^{-3}	Ecorr. mV	Icorr. (μA/cm^2)	Sample code
/	0.401	−210.1	1.37	A
79.8	0.081	−136.3	0.277	B
98.75	0.005	−684.4	0.01818	C

strength of the substrate with bioactive characteristics of HA which can persuade the ingrowths of the surrounding tissue of the bone and the future chemical bonding formation [32]. The improvement percentage of HA/TiO_2 composite coating samples in Ringer's solution are increased than (C) sample. The best improvement percentage for sample is (98.75%) at (C) sample.

4. Conclusion

Based on the obtained result, It was indicated that the layer growth of the TiO_2 on NiTi alloy as the base material followed by the MAO technique in quantified parameters has volcanic structures and circular microspores in rough was due to the continuous micro discharges that happened throughout the process. The Rutile and the anatase phases of the TiO_2 were presented on the material's surface after the XRD analysis. Therefore, it was recognized that the TiO_2 coating had grown on the surface of the material in crystal structure. To improve the bioactivity and corrosion resistance of NiTi alloy, the composite coating of HA/TiO_2 was equipped on a surface using one-step of MAO. The results of corrosion test in Ringer's solution observed that TiO_2-coated corrosion potentials, base material and HA/TiO_2-coated NiTi alloy were established to be as −136 mV, −210.1 mV and −684.4 mV, respectively. The densities of the current were determined as 1.37, 0.277 and 0.01818 μA/cm^2, respectively. Finally, it has been noticed that the composite coating of HA/TiO2 decreases the current density and increases the corrosion potential.

Declaration of Competing Interest

The authors declare that they have no known competing financial interests or personal relationships that could have appeared to influence the work reported in this paper.

References

[1] B. Clarke, W. Carroll, Y. Rochev, M. Hynes, D. Bradley, D. Plumley, Influence of nitinol wire surface treatment on oxide thickness and composition and its subsequent effect on corrosion resistance and nickel ion release, J. Biomed. Mater. Res. 79A (1) (2006) 61–70.
[2] G.C. McKay, R. Macnair, C. MacDonald, M.H. Grant, Biomaterials 17 (1996) 1339.
[3] D.J. Wever, A.G. Veldhuizen, D.J. Vries, Biomaterials 19 (1998) 761.
[4] H.C. Jiang, L.J. Rong, Effect of hydroxyapatite coating on nickel release of the porous NiTi shape memory alloy fabricated by SHS method, Surf. Coat. Tech. 201 (3-4) (2006) 1017–1021.
[5] US FDA Workshop - Cardiovascular Metallic Implants: Corrosion, Surface Characterization, and Nickel Leaching, March 8-9, 2012.
[6] Z. Cui, H. Man, X. Yang, The corrosion and nickel release behavior of laser surface- melted NiTi shape memory alloys in Hanks solution, Surf. Coat. Technol. 192 (2005) 347–353.
[7] J. Sui, W. Cai, Effect of diamond-like carbon (DLC) on the properties of the NiTi alloy, Diamond Relat. Mater. 15 (2006) 1720–1726.
[8] D.E. Allie, C.J. Hebert, C.M. Walker, Nitinol stent fractures in the SFA, Endovasc. Today 7 (2004) 22–34.
[9] M.M. Silva, L. Pichon, M. Drouet, J. Otubo, Roughness studies of NiTi shape memory alloy treated by nitrogen plasma based ion implantation at high temperatures, Surf. Coat. Technol. 211 (2012) 209–212.
[10] Havıtcxıoğ lu H. Improving surface properties of implant materials. J TOTBI_D 2011; 10: 178–183.
[11] J.L. Xu, F. Liu, F.P. Wang, D.Z. Yu, L.C. Zhao, Microstructure and corrosion resistance behavior of ceramic coatings on biomedical NiTi alloy prepared by micro-arc oxidation, Appl. Surf. Sci. 254 (20) (2008) 6642–6647.
[12] Raghuvir Singh, Narendra B. Dahotre, Corrosion degradation and prevention by surface modification of biometallic materials, J. Mater. Sci. Mater. Med. 18 (5) (2007) 725–751.
[13] Y.W. Gu, B.Y. Tay, C.S. Lim, M.S. Yong, Characterization of bioactive surface oxidation layer on NiTi alloy, Appl. Surf. Sci. 252 (5) (2005) 2038–2049.
[14] E. Arslan, Y. Totik, E.E. Demirci, Y. Vangolu, A. Alsaran, I. Efeoglu, High temperature wear behavior of aluminum oxide layers produced by AC micro arc oxidation, Surf. Coat. Technol. 204 (6-7) (2009) 829–833.
[15] Cuicui Wang, Feng Wang, Yong Han, Structural characteristics and outward–inwardgrowth behavior of tantalum oxide coatings on tantalum by micro-arcoxidation, Surf. Coat. Technol. 214 (2013) 110–116.
[16] F.C. Ma, P. Liu, Y. Chen, W. Li, X.K. Liu, X.H. Chen, D.H. He, Variousmorphologies hydroxyapatite crystals on Ti MAO film prepared byhydrothermal treatment, Phys. Proc. 50 (2013) 442–448.
[17] Kang Lee, Yong-Hoon Jeong, Yeong-Mu Ko, Han-Cheol Choe, William A. Brantley, Hydroxyapatite coatingon micropore-formed titanium alloy utilizing electrochemical deposition, Thin Solid Films 549 (2013) 154–158.
[18] Cora Vasilescu, Monica Popa, Silviu Iulian Drob, Petre Osiceanu, Mihai Anastasescu, Jose M. Calderon Moreno, Deposition and characterization of bioactive ceramic hydroxyapatite coating on surface of Ti–15Zr–5Nb alloy, Ceram. Int. 40 (9) (2014) 14973–14982.
[19] Shimin Liu, Xianjin Yang, Zhenduo Cui, Shengli Zhu, Qiang Wei, One-step synthesis of petal-like apatite/titania composite coating on a titanium by micro-arc oxidation, Mater. Lett. 65 (6) (2011) 1041–1044.
[20] N. Naresh, T. Vreeland, T.J. Ahrens, Microstructural modifications in a dynamically consolidated microcrystalline nickel– titanium alloy powder, J. Mater. Sci. 22 (1987) 4446–4452.
[21] D. Wei, Y. Zhou, Bioactive Microarc Oxidized TiO2-based Coatings for, Biomedical Implication (2011).
[22] Muhammad Qadir, Yuncang Li, Khurram Munir, Cuie Wen , Calcium Phosphate-Based Composite Coating by Micro-Arc Oxidation (MAO) for Biomedical Application: A Review, VOL. 43, NO. 5, 392–416,(2018).
[23] H.R. Wanga, F. Liub, Y.P. Zhangb, D.Z. Yuc, F.P. Wanga, Preparation and properties of titanium oxide film on NiTi alloy by micro-arc oxidation (2011).
[24] M.M. Shalabi, J.G. Wolke, V.M. Jansen, Evaluation of bone response to titanium – coated polymethacrylate resin (PMMA)implants by X-ray tomography, J. Mater sci. Mater. Med. 18 (2007) 2033–2039.
[25] K.W. Ng, H.C. Man, T.M. Yue(2011) 'characterization and corrosion study of Ni Ti laser surface alloyed with Nb or Co',vol. 257,Isaue.8,32 G9..
[26] Shimin Liua, Baoe Lib, Chunyong Liangb, Hongshui Wangb, Zhixia Qiao, Formation mechanism and adhesive strength of ahydroxyapatite/TiO2 composite coating on a titanium surface prepared by micro-arc oxidation (2015).
[27] A.A. Atiyah, A.K. Abid Ali, N.M. Dawood, Characterization of NiTi and NiTiCu porous shape memory alloys prepared by powder metallurgy (Part I), Arab. J. Sci. Eng. 40 (3) (2015) 901–913.
[28] Xuelin Zhang, Yufeng Zhang, Limin Chang, Zhaohua Jiang, Zhongping Yao, Xiaowei Liu, Effects of frequency on growth process of plasma electrolytic oxidation coating, Mater. Chem. Phys. 132 (2-3) (2012) 909–915.
[29] Parfenov EV, Yerokhin AL and Matthews A. Frequency response studies for the plasma electrolytic oxidation process. Surf Coat Tech 2007; 201(21): 8661–8670. E. E. Sukuroglu, S. Sukuroglu, K. Akar, Y.Totik.
[30] I. Efeoglu, E. Arslan, The effect of TiO2 coating on biological NiTi alloys after micro-arc oxidation treatment for corrosion resistance, J. Eng. Med. (2017).
[31] S. Ajay, R. Abhinandan, Study of hydroxyapatite and hydroxyapatite-chitosan composite coatings on stainless steel by electrophoretic deposition method, National Institute of Technology, 2010.
[32] A.K. Rajih, N.M. Dawood, F.S. Rasheed, Corrosion protection of 316 L stainless steel by HA coating via pulsed laser deposition technique, J. Eng. Appl. Sci. 13 (24) (2018) 10221–10231.